Successful imaging of land hydrophone and dual sensor data in a dry desert environment

Roy Burnstad, Andrey Bakulin, Mike Jervis, EXPEC Advanced Research Center, Saudi Aramco; Dmitry Alexandrov, St. Petersburg State University*

Summary

Hydrophones show a lot of promise as permanent single sensors for land seismic monitoring due to their potential to reject shear wave energy; however, a key issue in desert environment is their performance in dry rock above the water table. To investigate this issue a feasibility study was conducted over a producing oil field in Saudi Arabia. Results presented here include comparable images of colocated geophones, hydrophones and two distinct dual sensor applications. Conclusions indicate dry hydrophones can produce similar or slightly better images to geophones while dual-sensor summation delivers superior results over either individual dataset. Though challenges such as hydrophone coupling remain, the results are encouraging enough to seek improved dry hydrophone packaging and deployment methods, which can address both image and repeatability requirements.

Introduction

Use of hydrophones in seismic acquisition is well established for wet environments such as offshore, onshore below the water table and in vertical seismic profiling. An important benefit of hydrophone recording is the ability to conduct wavefield separation by combining it with geophone recording or so called dual-sensor summation (Barr and Sanders, 1989). When data is subject to different levels of noise then adaptive methods are required (Brittan and Starr, 2003). For permanent land monitoring, Meunier et al., (2001) demonstrated that cementing vertical 4C antennae with hydrophones inside kerosene-filled plugs produces reasonable results and allows wavefield separation when combined with the geophone; however, no images were produced because of sparse receiver coverage. Schissele et al. (2009) showed that hydrophones, buried at shallow depths below the water table, are less sensitive to shear waves and other noise and speculated that pre-stack hydrophone records may be more suitable for permanent monitoring with permanent sources. Land hydrophone studies to date have not shown any images and were only for hydrophones buried inside water-saturated formations where hydrophones are generally well coupled.

In this study we present the first examples of seismic images obtained with dual sensors in a dry desert environment where hydrophones are cemented above the water table. Despite initially low expectations and serious coupling challenges we demonstrate that hydrophones provide a distinct response different from geophones. After careful processing we observe clear improvements in dual-sensor 2D images compared to geophone images, thereby bringing marine ocean-bottom imaging technology to onshore in a dry environment. We also show how virtual source redatuming technology (Bakulin and Calvert, 2004) can be integrated with dual sensors.

Field data

A feasibility study for permanent seismic monitoring was conducted in a producing oil field in Saudi Arabia to evaluate various source and receiver acquisition configurations. The target horizon is located at depth of 2 km. A 2D line of 80 receiver stations was installed with colocated geophones and hydrophones cemented in vertical boreholes spaced every 30 m with sensors at depths up to 50 m below surface. Each receiver station comprises bunched geophones covered with sand at the surface along with three more sensor levels (10, 20 and 30 m), each level with a vertical geophone and a conventional hydrophone. As part of a repeatability study the 2D line is acquired with a single surface vibrator six times over a period of four months. Dense 3D areal shooting (7.5 m inline and 7.5 m crossline) is performed for efficient linear and scattered noise removal as well as for use in virtual source redatuming of surface sources to a 30 m receiver level.

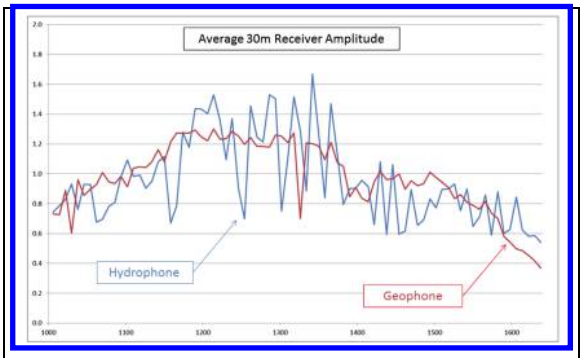

Figure 1. Average receiver amplitude from surface-consistent analysis. Colocated hydrophones and geophones at 30 m depth are input to a least-squares analysis. The horizontal axis is receiver station and vertical axis is average amplitude normalized to unity. Dry hydrophone station-to-station coupling (blue line) varies by as much as ±40% compared to geophone amplitude (red line).

DOI http://dx.doi.org/10.1190/segam2012-0957.1

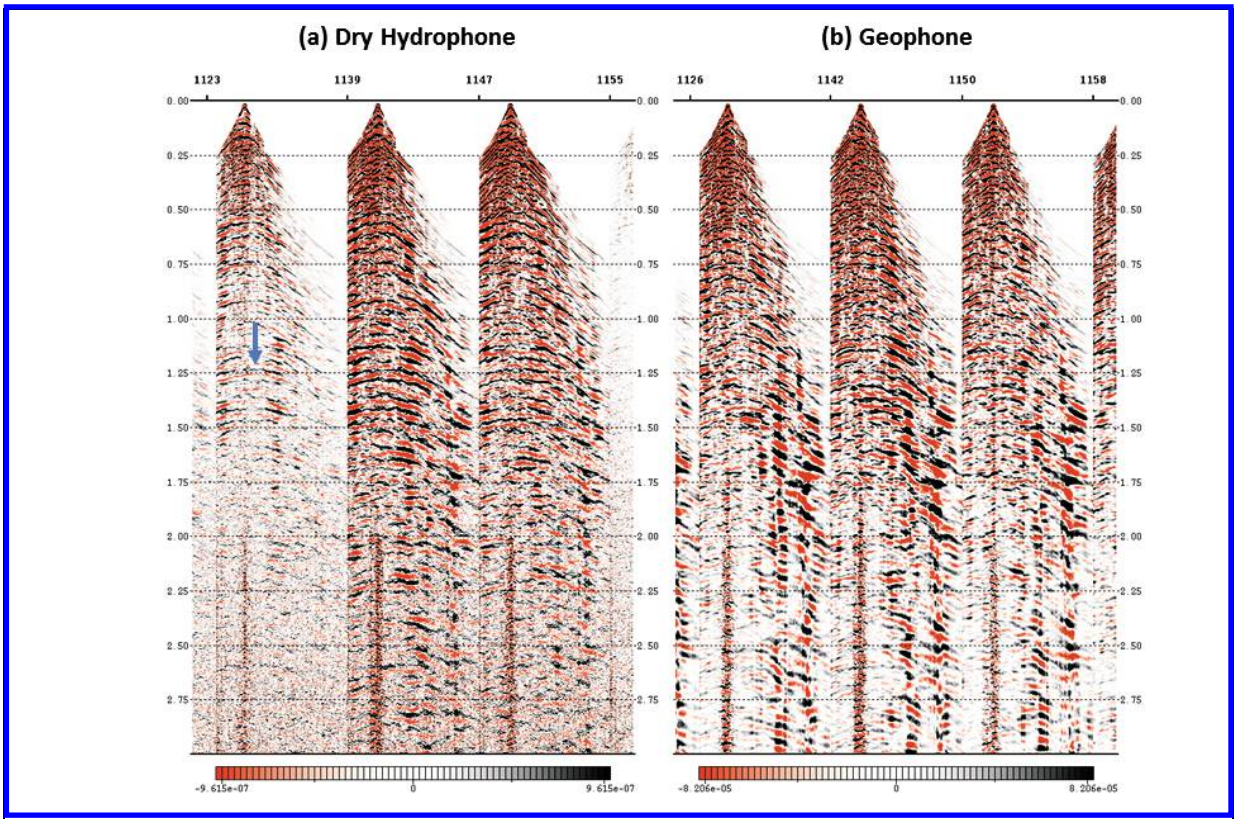

Figure 2. Representative common-receiver gathers for colocated hydrophone and geophones at 30 m depth after crossline diversity stack and FK filter. A time range of 0 to 3 s is displayed with timing lines every 250 ms. Dry hydrophone gathers (a) show variable amplitude and variable signal-to-no ise ratio. Geophone gathers (b) show consistent coupling and generally poorer S/N ratio, possibly due to higher levels of shear-wave noise being recorded. The target reflection at 1.25 s is visible on the dry hydrophone gathers [blue arrow in panel (a)].

Common-receiver gather displays and coupling scalars were used to compare hydrophone and geophone data. As expected hydrophone data are lower amplitude than the colocated geophones. Based on surface-consistent amplitude analysis, hydrophones show significantly more station-to-station coupling differences (Figure 1). Note that coupling scalars are computed simultaneously for all source, hydrophone and geophone locations. Corresponding receiver gather displays (Figure 2) confirm the surface-consistent amplitude analysis. Though coupling varies, dry hydrophone gathers (Figure 2a) show target reflections with single fold. Colocated geophones, while more consistently coupled, show a consistently poorer signal-to-noise ratio (Figure 2b) possibly due to increased sensitivity to low-frequency converted shear energy visible at the far offsets. We feel this indicates a great potential in dry hydrophone data provided consistent station-to-station coupling can be achieved.

Dual-sensor processing

Hydrophone and geophone data are processed through three stages: (1) noise removal, (2) summation, and (3) common-depth point (CDP) stack. The first stage is run in two steps. Step one is a common-receiver vertical stack of nine adjacent shot lines, which forms one output shot line with receivers spaced at 30 m. The vertical stack is run in diversity mode to attenuate both high-amplitude noise bursts and crossline-oriented scattered noise. The data are then sorted to receiver gathers and an FK filter is applied in two passes to remove both aliased and linear noise. Filtering in the common-receiver domain takes advantage of 7.5 m shot spacing. Receiver gathers are sorted in shot domain for the next processing stage. Both steps are independently run on the hydrophone and geophone datasets.

DOI http://dx.doi.org/10.1190/segam2012-0957.1

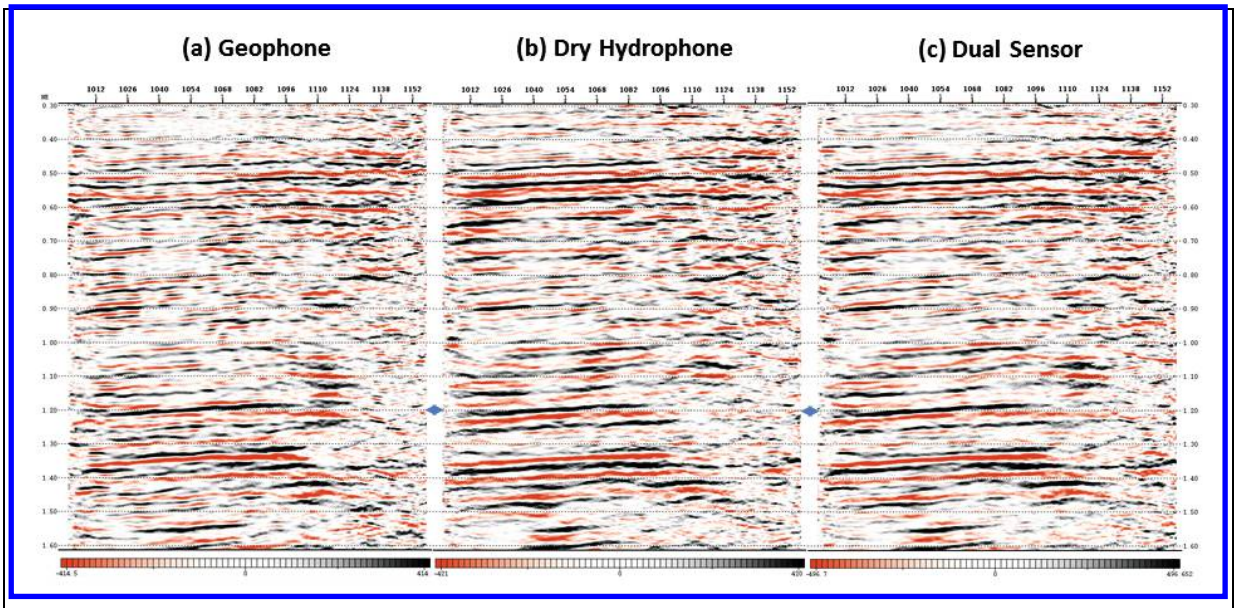

Figure 3. CDP stacks obtained with different sensors: (a) geophone, (b) dry hydrophone, and (c) dual sensor. Displayed time interval is from 300 ms to 1600 ms with timing lines every 100 ms. Target reflection (blue diamond) is imaged on all sections. The dual-sensor stack has the best continuity and wavelet character of all three sections.

The summation stage adds the colocated hydrophone and geophone shot records to output a deghosted record. Prior to summation the geophone trace is multiplied by a mean energy scalar calculated from a sliding time window on each dataset. The final geophone scalar is formed by dividing mean hydrophone energy by mean geophone energy. Several window lengths are tested to arrive at an output which optimally cancels ghost energy while mitigating the contribution of higher noise levels present on deeper portions of the hydrophone data. The last processing stage, CDP stack, is run on deghosted shot records. Steps within this stage include application of field statics, normal moveout, trace-by-trace amplitude balancing, mute and CDP stack. Field statics are calculated to redatum surface sources and buried receivers to a constant elevation equal to the nominal receiver elevation across the line. Amplitude balancing is applied independently to each trace based on four discrete 600 ms time windows. CDP stack is straight arithmetic sum followed by recovery scaling that result in an optimum amplitude balance between low- and high-fold portions of the stacked section.

Stacks of hydrophone and geophone data (Figure 3) show clear images of both shallow horizons and the target reflector located at around a two-way time of 1.2 s. The dual-sensor summation stack (Figure 3c) also shows good signal continuity and a sharper wavelet on several reflectors.

Quality of summation is also judged with amplitude spectra run on stacks of hydrophone, geophone and dual-sensor data (Figure 4). First, we observe opposite amplitude behavior of the hydrophone and geophone spectra near 40 Hz (Figure 4a and 4b). This is a good indication of receiver-side ghost energy. We also note a rapid roll off of low-frequency energy on the hydrophone spectra, again a good indication of ghost energy. The 35 to 45 Hz frequency range of dual summation stacks (Figure 4c) doesn't show the notch apparent on the hydrophone stack alone.

Dual-sensor and virtual-source processing

It has been shown that dual sensor summation is an important step that can greatly improve reflection images obtained after virtual source (VS) redatuming (Mehta et al., 2007). In this study we seek to demonstrate that land hydrophone and dual sensor has sufficient fidelity to achieve similar improvement. Input to VS processing are surface shot records surrounding a buried receiver. Noise removal is parameterized similar to the previous dual-sensor sequence with the exception of no crossline vertical stack. An output VS record is a shot/offset gather representing the input surface shot records redatumed to the buried receiver level. VS redatuming is applied separately to hydrophone and geophone datasets prior to dual-sensor summation. We note that dual-sensor summation for virtual source data is not performed the same as normal summation. That is, deghosted output is achieved by subtracting geophone from hydrophone instead of adding

DOI http://dx.doi.org/10.1190/segam2012-0957.1

geophone to hydrophone. This requirement can be explained by reversed polarity of downgoing energy on the hydrophone and geophone, being correlated with the same polarity upgoing reflections, resulting in polarity reversed hydrophone and geophone reflections after separate correlation stack of each dataset.

VS shot record processing completes with a CDP stack including application of field statics, normal moveout, trace-by-trace amplitude balancing, mute and CDP stack. The shot field statics are adjusted to reflect the new datum level of each virtual source. Geophone, dual sensor and VS dual-sensor stacks are compared for signal and wavelet quality (Figure 5). All three stacks show good reflector continuity. The dual sensor stacks show improved wavelet character on several reflectors.

Discussion and conclusions

This experiment shows that compared to geophones, dry cemented hydrophones are inconsistently coupled. Signal-to-noise ratio permitting, visible reservoir reflections can be observed on single-fold hydrophone records. We demonstrated that dry hydrophones can produce similar images to geophones while dual-sensor summation delivers superior results over either individual dataset. The results are encouraging enough to seek a commercial dry land hydrophone sensor with robust deployment methods, which can address both image and repeatability requirements. There is good indication from this experiment that coupling issues can be resolved; for example in ongoing studies we have observed more consistent hydrophone coupling from 4C sensors, thereby indicating that packaging is an important factor.

Acknowledgments

We would like to thank Saudi Aramco for allowing us to publish this work and CGGVeritas and ARGAS (Arabian Geophysical and Surveying Company) for dedication in executing the field work.

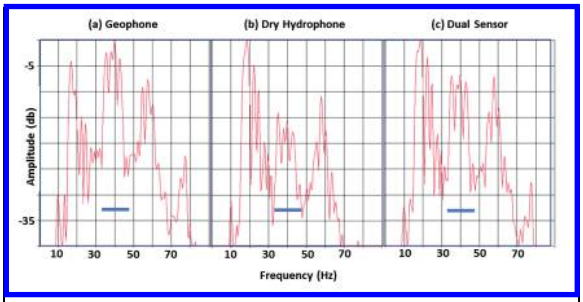

Figure 4. Amplitude spectra from shallow window on stacks displayed in Figure 3. Horizontal scale is frequency and vertical scale is amplitude in db. Complementary behavior in 35-45 Hz range (blue bar) on geophone (a) and dry hydrophone (b) indicating the presence of ghost energy. Dual sensor spectra (c) is relatively well balanced.

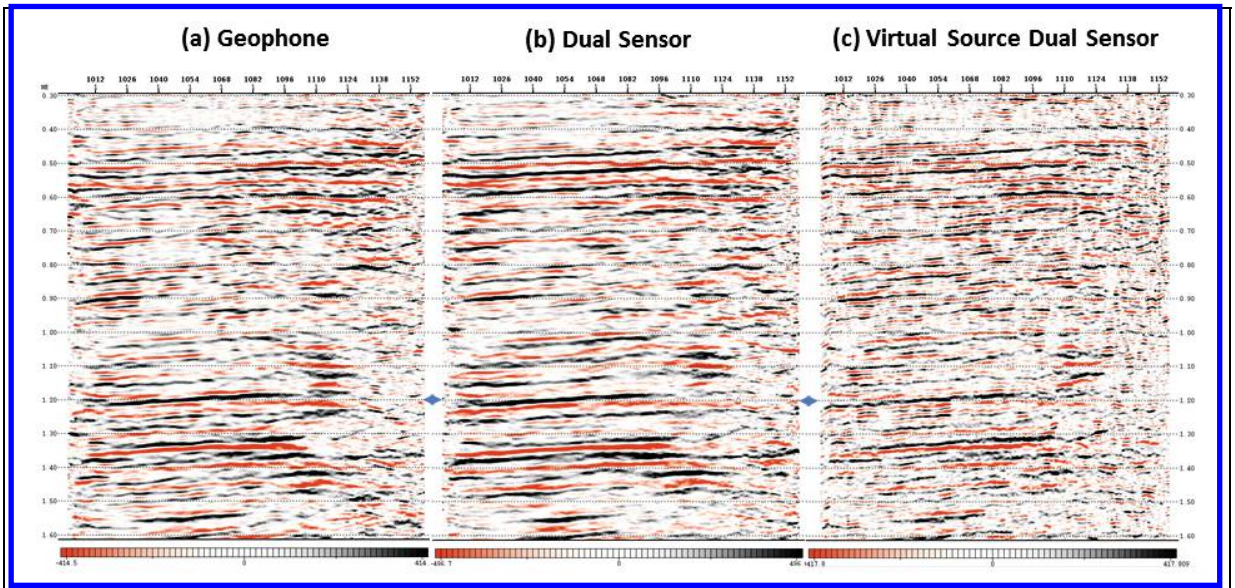

Figure 5. Comparison of various CDP stacks: (a) geophone, (b) dual sensor, (c) virtual source obtained after wavefield separation with dual sensor. Displayed time interval 300 ms to 1600 ms, timing lines every 100 ms. Target reflection (blue diamond) is imaged on all sections. The dual-sensor stack has the best continuity while the VS stack exhibits better resolution with a more compressed wavelet.

DOI http://dx.doi.org/10.1190/segam2012-0957.1

http://dx.doi.org/10.1190/segam2012-0957.1

EDITED REFERENCES

Note: This reference list is a copy-edited version of the reference list submitted by the author. Reference lists for the 2012 SEG Technical Program Expanded Abstracts have been copy edited so that references provided with the online metadata for each paper will achieve a high degree of linking to cited sources that appear on the Web.

REFERENCES

Bakulin, A., and R. Calvert, 2004, Virtual source: New method for imaging and 4D below complex overburden: 74th Annual International Meeting, SEG, Expanded Abstracts, 2477–2480.

Barr, F. J., and J. I. Sanders, 1989, Attenuation of water-column reverberations using pressure and velocity detectors in a water-bottom cable: 59th Annual International Meeting, SEG, Expanded Abstracts, 653–656.

Brittan, J., and J. Starr, 2003, Applications of adaptive noise attenuation to dual sensor seismic data: 73rd Annual International Meeting, SEG, Expanded Abstracts, 865–868.

Mehta, K., A. Bakulin, J. Sheiman, R. Calvert, and R. Sneider, 2007, Improving the virtual source method by wavefield separation: Geophysics, **74**, no. 4, V79–V86.

Meunier, J., F. Huguet, and P. Meynier, 2001, Reservoir monitoring using permanent sources and vertical receiver antennae: The Céré-la-Ronde case study: The Leading Edge, **20**, 622–629.

Schissele, E., E. Forgues, J. Echappé, J. Meunier, O. de Pellegars, and C. Hubans, 2009, Seismic repeatability — Is there a limit?: 71st Conference and Exhibition, EAGE, Extended Abstracts, V021.